JOURNAL OF GUIDANCE, CONTROL, AND DYNAMICS
Vol. 31, No. 1, January–February 2008

Study on Relative Orbit Geometry of Spacecraft Formations in Elliptical Reference Orbits

Fanghua Jiang,* Junfeng Li,† Hexi Baoyin,‡ and Yunfeng Gao§
Tsinghua University, 100084 Beijing, People's Republic of China

DOI: 10.2514/1.30394

This paper studies the relative orbit geometry of a leader–follower spacecraft formation flying in unperturbed elliptical reference orbits. The first-order relative position equations, derived using the reference orbital element approach under the condition that the follower and leader spacecraft have equal semimajor axes, are transformed from trigonometric forms to parametric and algebraic forms. The conditions for and the number of self-intersections of the relative orbit projected onto the three coordinate planes of the leader local-vertical–local-horizontal frame are obtained. The relative orbit proves to be three-dimensional instead of planar in most cases, and may self-intersect spatially at most once. The collision between the follower and leader spacecraft corresponds to the case where the solution curve to the first-order relative motion equations passes through the origin. The conditions for collision are subsequently determined. For a nondegenerate case (in which none of the relative motion in the radial, in-track, and cross-track directions vanish), three types of relative orbit are possible. Most frequently, the relative orbit is on a one-sheet hyperboloid. Otherwise, when the relative orbit has a real or finite imaginary self-intersection, it rests on an elliptic cone. In the rest of the cases, including that with an imaginary self-intersection at infinity, the relative orbit is on an elliptic cylinder. The criteria for these three types are given, respectively, followed by examples.

Nomenclature

a	=	semimajor axis
a_{ij}	=	coefficient of a quadric surface equation
c_j	=	the jth parameter with respect to orbit element differences
d_j	=	the jth integration constant in the periodic solutions of Lawden's equations
e	=	eccentricity
f	=	true anomaly
I_j	=	the jth invariant of a quadric surface
i	=	orbit inclination
K_2	=	semi-invariant of a quadric surface
k_j	=	the jth ratio between two certain parameters c_j
M	=	mean anomaly
m	=	sum of two distinct values of s
n	=	product of two distinct values of s
r	=	distance from the Earth's center to the leader spacecraft
s	=	variable with respect to true anomaly
u_j	=	the jth eigenvalue of the characteristic equation of a quadric surface
X_j	=	the jth eigenvector of the characteristic equation of a quadric surface
x, y, z	=	follower relative state vector in the leader LVLH frame
Δ	=	discriminant, or difference symbol that appears with orbit elements
θ	=	argument of latitude
Ω	=	right ascension of the ascending node
ω	=	argument of perigee

Subscript

f	=	follower spacecraft

Superscript

r	=	reference orbit element

I. Introduction

MUCH research has been conducted on spacecraft formation flying, with the focus on the vital problem of modeling the relative motion. Owing to mainly three classes of perturbation: the nonlinearity of the differential gravitational acceleration, eccentricity of the reference orbit, and the Earth's oblateness, the relative motion of one spacecraft (termed the follower) with respect to another (termed the leader) is rather complex. In practice, various models handle the perturbation by different degrees of approximation.

The earliest model of relative motion was Hill's linear model [1] of the motion of the moon with respect to the sun–Earth system, based on the assumption of a circular reference orbit. Almost one century later, the Clohessy–Wiltshire (CW) linear model [2] described spacecraft relative motion on the same assumption. The CW equations and Hill's equations are unified in form and collectively named HCW equations, which have been generalized from first-order to second [3], third [4], and higher [5] orders. Meanwhile, the linearized differential equations describing the relative motion of spacecraft in unperturbed elliptical reference orbits were presented independently by Lawden [6] and the Tshauner–Hempel team [7], and consequently named Lawden's equations or Tschauner–Hempel equations. The singularity problem in the original solutions for Lawden's equations was later resolved by Carter [8]. Melton [9] derived the relative motion equations in the form of a series expansion in eccentricity. Aiming at the solutions of the linearized relative motion equations, Inalhan et al. [10] developed an initialization procedure for elliptical reference orbits. In all of these studies, the dynamic equations of relative motion ignored orbital perturbations such as the Earth's oblateness, which was taken into account by other researchers such as Schaub and Alfriend [11], and Gim and Alfriend [12,13]. In addition to Cartesian coordinates, canonical coordinates [14] and spherical coordinates [15] have also been used to model spacecraft relative motion, derive second-order solutions, or handle the Earth's oblateness. To avoid solving the

Received 12 February 2007; revision received 26 June 2007; accepted for publication 26 June 2007.

*Ph.D. Candidate, School of Aerospace; jiangfh04@mails.thu.edu.cn.
†Professor, School of Aerospace; lijunf@tsinghua.edu.cn.
‡Associate Professor, School of Aerospace; baoyin@tsinghua.edu.cn.
§Associate Professor, School of Aerospace; gaoyunfeng@tsinghua.edu.cn.

complex differential equations of relative motion, various geometric approaches that map relative motion coordinates to orbital element differences [12] or other metrics [16–20] have been presented. Among these is the method presented by Baoyin et al. [16] to describe relative motion based on relative orbital elements, which was used by Li et al. [17] and Meng et al. [18] to analyze the relative orbital configuration with and without the perturbation of the Earth's oblateness for slightly elliptical reference orbits. Wang et al. [19] also presented the reference orbital element (ROE) approach to describe relative motion on the celestial sphere, which was further developed by Jiang et al. [20].

The variety of models of spacecraft relative motion is considerable. Nevertheless, sufficient understanding in the general relative orbit geometry and configuration of the follower spacecraft flying around the leader in arbitrary elliptical orbits has not been achieved analytically. For circular as well as slightly elliptical reference orbits without perturbations, the relative orbit configurations are comparatively simple, such as a 2:1 ellipse in the radial/in-track plane [16,17]. One example was the detailed analysis of a class of formations with constant configuration in the in-track/cross-track plane presented by Hughes and Hall [21]. Meanwhile, for highly elliptical orbits, it is difficult to obtain analytic solutions of relative orbit configuration. Li et al. [17] used simulations to study the relative configurations for elliptical reference orbits with and without J_2 perturbation. On the other hand, Jiang et al. [20], by expanding the relative motion in the radial/in-track plane into Fourier series whose amplitudes formed a geometric sequence, developed a method to approximate the relative orbit with an ellipse when appropriate. Schaub [22] analyzed the relative orbit geometry of a spacecraft formation in unperturbed elliptical orbits with orbit element differences. Divided by the radius of the leader spacecraft, the expressions of the linearized relative orbit coordinates are simplified into the addition of cosine and sine values of single and double of the true anomaly. Hence, it is trivial to determine the dimensionless solution to the relative orbit shape. However, the shape thus determined is not the true one because the radius of the leader spacecraft used in division is time dependent for an elliptical reference orbit. Similarly, Lane and Axelrad [23] obtained the expressions for the relative orbit coordinates in the cosine and sine values of the true anomaly and the eccentric anomaly. However, due to the eccentricity of the reference orbit, only three types of special formations could be designed analytically as the result of their research. In addition, Kholshevnikov and Vasiliev [24,25] analytically studied the minimum, maximum, and mean distance between two arbitrary elliptical orbits. Recently, Gurfil and Kholshevnikov [26] pointed out that for any arbitrary elliptical reference orbit, the relative motion solution always evolved on an invariant manifold, in particular on an elliptic torus when some relative orbit elements were very small. It is worth noting that in [24–26] the relative orbit radius is not constrained to small values alone.

In close formations, the relative distance between the leader and a follower spacecraft is small compared with their geocentric distances. If the second-order relative distance, i.e., the relative distance multiplied by the ratio of the relative distance to the geocentric distance of any spacecraft, is negligible, the relative motion of the follower with respect to the leader can be linearized, and the relative motion configuration space can be determined even more readily and specifically than in the research by Gurfil and Kholshevnikov [26]. There have been few reported efforts to understand the geometrical structure of the relative orbit in the general case of spacecraft close formation in arbitrary elliptical orbits. In particular, it is not known what conditions the orbit elements should satisfy in order for the relative orbit projected onto the coordinates plane to be figure-eight shaped as shown in [10], the maximum number of times the projected curve can intersect with itself, whether or not the relative orbit is planar, whether and how the relative orbit can intersect with itself spatially, and so on. In [23], Lane and Axelrad stated without supporting details that, in general, the relative orbit with an elliptical reference orbit would not be an ellipse in any plane. Their conclusion will be explained in this paper with algebraic methods. Our mathematical derivation will shed light on the inherent characters of relative motion of spacecraft formation, and show that formation design is not constrained to the special cases presented in [23].

This paper, therefore, aims at making two main contributions. First, we reveal the geometrical characters of the relative orbit projected onto the three coordinate planes of the leader local-vertical–local-horizontal (LVLH) frame with algebraic methods. We begin with the first-order relative position equations (FRPE) expressed in the leader LVLH frame in [20]. These equations were obtained in terms of orbit element differences with the ROE approach [19,20] modeling unperturbed relative motion under the condition that the follower and leader spacecraft have equal semimajor axes. Treating the tangent value of half the true anomaly as an independent variable, and replacing the orbit element differences with appropriate parameters, we transform the FRPE from trigonometric forms into algebraic forms, which are also applicable to the study of the periodic solutions of Lawden's equations presented by Inalhan et al. [10] with proper parameterization of the integration constants. On the basis of these two important transformations, we are able to apply these algebraic equations to the general characters of the relative orbit projected onto the three coordinate planes of the leader LVLH frame using algebraic methods, which marks an essential departure from all the preceding references inevitably involving trigonometric functions in the relative motion equations. The results will indicate that the projections of the relative orbit are quartic curves, in accordance with the assertion in [23] that none of the projected curves is an ellipse. Furthermore, we discover that the projected curves may self-intersect at most once in the radial/cross-track plane, but twice in both the radial/in-track and in-track/cross-track planes. The conditions that these parameters should satisfy to achieve self-intersection are also determined, making it possible to design formations with special shapes such as figure-eight shapes in the coordinate planes.

Second, the algebraic FRPE reveals the spatial characters of the relative orbit geometry. The relative orbits prove to be three-dimensional in the majority of cases with elliptical reference orbits. Collision between the follower and the leader is examined. The result enables the avoidance of collision in formation designs. The relative orbits prove to be self-intersecting at most once, which corresponds to the formation design in which the follower spacecraft passes through a point twice in the leader LVLH frame, but no more than twice. Most important, applying the theory of quadric surfaces, we reveal that the relative orbits are always on quadric surfaces, most frequently on one-sheet hyperboloids, and in rare cases on elliptic cones or elliptic cylinders. This study differs from Gurfil and Kholshevnikov's [26] result that the relative orbit is on an elliptic torus, which is a quartic surface. A few cases will be included to substantiate the conclusions, and demonstrate that they are applicable to arbitrary elliptical reference orbits.

The scope of this paper bears restating. It only considers the geometry of relative orbit without perturbations or active controls. The relative orbit velocity is excluded from out interest. Spacecraft close formation is assumed, in which the relative distance between two spacecraft is so small that the associated second-order relative distance is negligible, and the relative position equations are consequently linearized. The semimajor axis of the follower is considered equal to that of the leader. The results thus obtained about relative orbit geometry are first-order approximations, and without active control formation configurations cannot be maintained in the presence of perturbations. Nevertheless, this work sheds light on the inherent characters of relative motion, and has the potential to reduce the control cost in the design of orbits.

II. Relative Motion Modeling

The ROE approach [19] essentially models the relative motion of the follower with respect to the leader, as well as their motions with respect to the Earth, on the celestial sphere. As shown in Fig. 1, we adopt the traditional Earth-centered-inertial frame $OXYZ$. The relative motion coordinates of the follower with respect to the leader LVLH frame $Lxyz$ are denoted by x, y, and z, in which the x axis

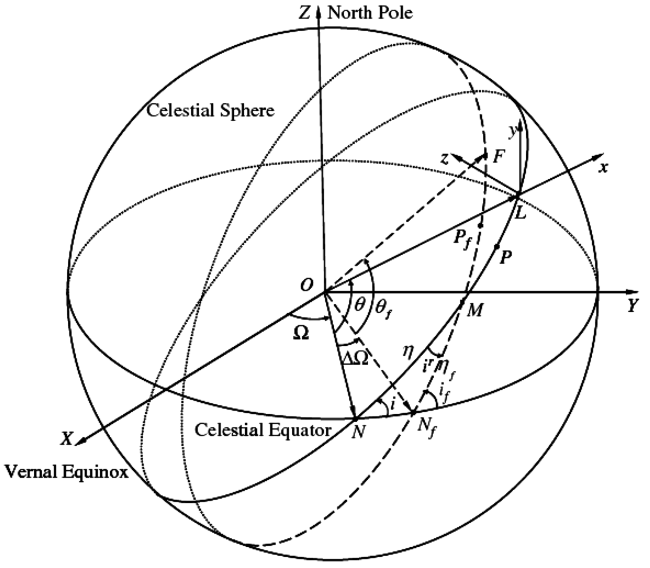

Fig. 1 Projections of the leader and follower orbits onto the celestial sphere.

points radially away from the Earth's center, the y axis points in the in-track direction with increasing true anomaly, and the z axis points in the cross-track direction. The projections of the leader and follower orbits, represented by the solid line and the broken line, respectively, intersect each other at M. They intersect the celestial equator at N and N_f, respectively. These three intersection points determine the spherical triangle NN_fM, of which the three vertex angles are i, $\pi - i_f$, and i^r, and the three arc distances are $\Delta\Omega$, η_f, and η. All of the angular metrics are defined as counterclockwise positive. The vertex angle i^r, termed the reference inclination, is the inclination angle between the orbital planes of the leader and follower. The arc distance from M to the leader's instantaneous position L is denoted by Ω^r, termed the reference ascension of the ascending node. Analogously, the arc distance from M to the follower's instantaneous position F is denoted by θ^r, termed the reference orbit angle. The perigees of the leader and the follower are denoted by P and P_f, respectively. With these notations, we can write that $\Omega^r = \theta - \eta$ and $\theta^r = \theta_f - \eta_f$, where θ and θ_f are the arguments of the latitude of the leader and the follower, respectively.

In terms of the preceding reference elements, the position coordinates of the follower with respect to the leader projected onto the leader LVLH frame are given by

$$\begin{cases} x = r_f(\cos\Omega^r\cos\theta^r + \sin\Omega^r\sin\theta^r\cos i^r) - r \\ y = r_f(-\sin\Omega^r\cos\theta^r + \cos\Omega^r\sin\theta^r\cos i^r) \\ z = r_f\sin\theta^r\sin i^r \end{cases} \tag{1}$$

where r and r_f refer to the scalar radii of the leader and the follower from the center of the Earth, respectively. In close formation without perturbations, where the leader and follower spacecraft are close to each other at all times, the semimajor axis of the follower is considered equal to that of the leader, and some quantities relating to the orbit element differences between the follower and the leader are small [20]. Then Eqs. (1) can be linearized as follows:

$$\begin{cases} x = -a\Delta e\cos f + \frac{a\Delta M}{\sqrt{1-e^2}}e\sin f \\ y = \frac{a\Delta M}{\sqrt{1-e^2}}(1+e\cos f) + a\Delta e\sin f\left(1+\frac{1}{1+e\cos f}\right) + \frac{a(1-e^2)(\Delta\omega+\Delta\Omega\cos i)}{1+e\cos f} \\ z = \frac{a(1-e^2)}{1+e\cos f}[(\Delta i\cos\omega + \Delta\Omega\sin\omega\sin i)\sin f + (\Delta i\sin\omega - \Delta\Omega\cos\omega\sin i)\cos f] \end{cases} \tag{2}$$

We term Eqs. (2) the first-order relative position equations (abbreviated as FRPE). Both Eqs. (1) and (2) are given here without derivation; the full details, as well as some other relationships between the angles and arc distances of the spherical triangle NN_fM, are available in [20]. Alternatively, Eqs. (2) can be found in [23] as equivalent to Eq. (12). Generally speaking, the difference of the mean anomaly ΔM is dependent on time, whereas it is constant in the case of $\Delta a = 0$. Hereafter, in this paper, it will be defaulted its initial value of $\Delta M = \Delta M_0$. For simplification, five new parameters are also defined as follows:

$$\begin{cases} c_1 = a\Delta e \\ c_2 = a\Delta M/\sqrt{1-e^2} \\ c_3 = a(1+e)(\Delta\omega + \Delta\Omega\cos i) \\ c_4 = a(1-e^2)(\Delta i\cos\omega + \Delta\Omega\sin\omega\sin i) \\ c_5 = a(1+e)(\Delta i\sin\omega - \Delta\Omega\cos\omega\sin i) \end{cases} \tag{3}$$

These definitions are elegant because the mapping from the set of orbit element differences $\{\Delta e, \Delta M, \Delta i, \Delta\Omega, \Delta\omega\}$ to the parameter set $\{c_1, c_2, c_3, c_4, c_5\}$ is one-to-one as long as the orbit elements of the leader are given with nonzero orbit inclination.

$$\begin{cases} \Delta e = c_1/a \\ \Delta M = c_2\sqrt{1-e^2}/a \\ \Delta i = [c_4\cos\omega + c_5(1-e)\sin\omega]/[a(1-e^2)] \\ \Delta\Omega = [c_4\sin\omega - c_5(1-e)\cos\omega]/[a(1-e^2)\sin i] \\ \Delta\omega = c_3/[a(1+e)] - [c_4\sin\omega - c_5(1-e)\cos\omega]/[a(1-e^2)\tan i] \end{cases} \tag{4}$$

Substituting Eqs. (4) into Eqs. (2) yields

$$\begin{cases} x = -c_1\cos f + c_2 e\sin f \\ y = c_2(1+e\cos f) + c_1\sin f\left(1+\frac{1}{1+e\cos f}\right) + \frac{(1-e)c_3}{1+e\cos f} \\ z = \frac{1}{1+e\cos f}[c_4\sin f + (1-e)c_5\cos f] \end{cases} \tag{5}$$

Because the FRPE (2) is 2π periodic in f, bounding f on the interval $[0, 2\pi)$ is sufficient to study the relative motion geometry. To study the equations of relative position, Eqs. (2), by algebraic method, replace the variable f with s, defined as

$$s = \tan(f/2), \qquad f \in [0, 2\pi) \tag{6}$$

which yields $\cos f = (1-s^2)/(1+s^2)$ and $\sin f = 2s/(1+s^2)$. Then, adopting Eqs. (3), we rebuild Eqs. (5) as

$$\begin{cases} x = c_1 + \frac{2(ec_2 s - c_1)}{s^2+1} \\ y = (1-e)c_2 + c_3 + \frac{2(c_1 s + ec_2)}{s^2+1} + \frac{2(c_1 s - ec_3)}{(1-e)s^2+1+e} \\ z = -c_5 + \frac{2(c_4 s + c_5)}{(1-e)s^2+1+e} \end{cases} \tag{7}$$

Because the interval of f is $[0, 2\pi)$, the mapping from f to s in Eq. (6) is not continuous only at the point $f = \pi$. s tends to $+\infty$ as f tends to π^-; whereas s tends to $-\infty$ as f tends to π^+. We combine the two values $+\infty$ and $-\infty$ to one value ∞ to make this mapping continuous and one-to-one, because both $s = +\infty$ and $s = -\infty$ give the same set of relative motion coordinates in Eqs. (7). The algebraic

Eqs. (7), where $0 \le |s| \le \infty$, are hence equivalent to the FRPE (2) in the study of the relative orbit geometry.

The linearized relative motion equations for spacecraft in elliptical orbits without perturbations were first presented by Lawden [6], and named Lawden's equations. The solutions to Lawden's equations were subsequently studied more thoroughly and perfected by many researchers [8–10]. A set of periodic solutions can be written as [10]

$$\begin{cases} x = -d_3 \cos f + d_1 e \sin f \\ y = d_1(1 + e\cos f) + d_3 \sin f\left(1 + \frac{1}{1+e\cos f}\right) + \frac{d_4}{1+e\cos f} \\ z = \frac{d_5 \sin f}{1+e\cos f} + \frac{d_6 \cos f}{1+e\cos f} \end{cases} \tag{8}$$

where the integration constants can be expressed in terms of initial ($f = 0$) relative position (x_0, y_0, z_0) and initial relative velocity (x_0', y_0', z_0') as

$$\begin{aligned} &d_1 = \frac{x_0'}{e}, \qquad d_2 = \frac{(1+e)^2}{e^2}[(2+e)x_0 + (1+e)y_0'], \\ &d_3 = -\frac{1+e}{e}(2x_0 + y_0') \qquad d_4 = \frac{1+e}{e}[-(1+e)x_0' + ey_0], \\ &d_5 = (1+e)z_0', \qquad d_6 = (1+e)z_0 \end{aligned} \tag{9}$$

where $(\cdot)'$ denotes the derivative of $(\cdot)$ with respect to f, observed in the leader LVLH frame. Note that the second integration constant d_2 does not appear in Eqs. (8) because it necessarily equals zero for the solutions to be periodic.

Equations (8) can also be transformed into Eqs. (7) by replacing f with s through Eq. (6), and $\{d_1, d_3, d_4, d_5, d_6\}$ with $\{c_1, c_2, c_3, c_4, c_5\}$ through

$$\begin{aligned} d_1 = c_2, \qquad d_3 = c_1, \qquad d_4 = (1-e)c_3 \\ d_5 = c_4, \qquad d_6 = (1-e)c_5 \end{aligned} \tag{10}$$

Therefore, the algebraic Eqs. (7) are also applicable to the study of the periodic solutions of Lawden's equations. The parameters $\{c_1, c_2, c_3, c_4, c_5\}$ can express not only orbit element differences through Eqs. (3) but also Cartesian initial relative position and velocity through Eqs. (9) and (10).

III. Relative Orbit Projected onto the Coordinate Planes

The FRPE have been presented in algebraic form as Eqs. (7) in the preceding section. The following two sections will describe the use of these equations to study the relative orbit geometry by algebraic method. There is no doubt that under the condition $\Delta a = 0$, the precise relative orbit expressed by Eqs. (1), and the first-order relative orbit expressed by Eqs. (2) or Eqs. (7), are both closed curves. This leads to the question on the specific structure of this closed curve, especially when projected onto the three coordinate planes of the leader LVLH frame. This section answers whether and how many times the projected curves of a relative orbit self-intersect. Here, a curve is termed self-intersected if it passes through a point no less than twice, and this point is termed the self-intersection point of the curve.

In Eqs. (7), let $x = z$, and a quartic equation in the variable s is obtained. That is to say, the relative orbit is generally a quartic curve when projected onto the radial/cross-track plane. Analogously, the relative orbit is also a quartic curve when projected onto the radial/in-track or in-track/cross-track planes. If a curve expressed by a set of single-parameter equations self-intersects, there must be at least two different values of the parameter mapping the same set of coordinates. In Eqs. (7), regarding x as given, the first equation can be transformed into a quadratic equation with respect to s, with two different values of s, s_1 and s_2, yielding the same value of x. We thus obtain

$$c_1 + \frac{2(ec_2 s_1 - c_1)}{s_1^2 + 1} = c_1 + \frac{2(ec_2 s_2 - c_1)}{s_2^2 + 1} \tag{11}$$

namely

$$\frac{(s_2 - s_1)[ec_2 s_1 s_2 - ec_2 - c_1(s_2 + s_1)]}{(s_1^2 + 1)(s_2^2 + 1)} = 0 \tag{12}$$

Because s_1 and s_2 are different, $s_2 - s_1$ must be nonzero, and therefore omitted from Eq. (12). Replacing s_1 and s_2 with m and n through the formulas

$$m = s_1 + s_2, \qquad n = s_1 s_2 \tag{13}$$

we reduce Eq. (12) to

$$c_1 m - ec_2(n-1) = 0 \tag{14}$$

Similarly, the relationships about the y and z components can be derived as

$$\frac{ec_2 m + c_1(n-1)}{m^2 + (n-1)^2} = \frac{e(1-e)c_3 m - c_1[(1-e)n - (1+e)]}{(1-e^2)m^2 + [(1-e)n - (1+e)]^2} \tag{15}$$

and

$$(1-e)c_5 m + c_4[(1-e)n - (1+e)] = 0 \tag{16}$$

In order for s_1 and s_2 to be real and unequal, m and n should satisfy the discriminant

$$m^2 - 4n > 0 \tag{17}$$

Equations (14–17) will be useful to study the self-intersection of the relative orbit as well as its projected curves.

A. Projection onto the Radial/Cross-Track Plane

When the relative orbit projected onto the radial/cross-track plane self-intersects, Eqs. (14), (16), and (17) are satisfied. It is not difficult to solve linear Eqs. (14) and (16) with respect to m and n. Substitution of the consequent solutions into Eq. (17) yields the discriminant of self-intersection

$$e^4 c_2^2 c_4^2 - e^2(1-e)^2 c_2^2 c_5^2 - (1-e^2)c_1^2 c_4^2 - 2e(1-e)c_1 c_2 c_4 c_5 > 0 \tag{18}$$

which shows the condition that parameters $c_j (j = 1, 2, \ldots, 5)$ satisfy to make the projected curve self-intersect. If necessary, this condition can be expressed in terms of orbit elements through Eqs. (3). Because a set of two linear equations with two variables have at most one set of solutions, the projected curve self-intersects at most once. To simplify the inequality (18), we define three ratios with respect to $c_j (j = 1, 2, \ldots, 5)$ as follows:

$$k_1 = c_1/(ec_2), \qquad k_2 = c_3/[(1+e)c_2], \qquad k_3 = c_5/c_4 \tag{19}$$

Note that although c_3 does not appear in this immediate context, the ratio k_2 will be used in the later discussion. Then, the inequality (18) can be written as

$$\Delta_1 = [(1-e)k_3 + (1+e)k_1](k_3 + k_1) - e^2/(1-e) < 0 \tag{20}$$

where the left side of the less-than sign is denoted by Δ_1. Obviously, only if the eccentricity e is in the interval (0, 1), the equation $\Delta_1 = 0$ corresponds to a hyperbola with regard to k_1 and k_3. It is not difficult to show the graph of the discriminant of self-intersection on the x–z plane as in Fig. 2, in which e is set to be 0.5 as an example. The coordinates of points A and B are $[0, e/(1-e)]$ and $[e/(1-e^2)^{0.5}, 0]$, respectively. The graph is symmetrical across the origin. The projected curve of the relative orbit will not self-intersect if the parameters are in the white area, whereas it will intersect once in the shaded area. Points 1, 2, 3, and 4 are sample points of the example given at the end of this section. The values of s and the coordinates at the self-intersection point can be obtained by first solving Eqs. (14)

and (16). The true anomaly f at the self-intersection point can also be evaluated by using $s = \tan(f/2)$.

B. Projection onto the Radial/In-Track Plane

When the relative orbit projected onto the radial/in-track plane self-intersects, Eqs. (14), (15), and (17) are satisfied. Expressing m with n through Eq. (14), substituting the consequent expression into Eqs. (15) and (17), and using Eqs. (19), we obtain

$$\begin{cases} (1-e)[(2-e)k_1^2 + (1+e)(1-k_2)]m^2 - 2e(3-2e)k_1 m + 4e^2 = 0 \\ m^2 - 4k_1 m - 4 > 0 \end{cases} \tag{21}$$

The relationship between the existing solution and the coefficients of this type of system of equation are given with derivations in the Appendix; only the conclusion is presented here. After the discriminants Δ_0, Δ_1, Δ_2, and Δ_3 are obtained as Eqs. (A10) in the Appendix, the conditions for the projected curve with two self-intersection points can be written as

$$(\Delta_1 > 0) \cap (\Delta_2 > 0) \cap (\Delta_3 > 0) \tag{22}$$

the conditions for no self-intersection point as

$$[(\Delta_0 \neq 0) \cap (\Delta_1 \geq 0) \cap (\Delta_2 \geq 0) \cap (\Delta_3 \leq 0)] \cup [\Delta_1 < 0] \tag{23}$$

and for one self-intersection point, k_1 and k_2 satisfy the complement of the combined conditions of (22) and (23).

The discriminants are depicted in Fig. 3, which is representative of general cases with $e = 0.5$ as a specific example. Point D with coordinates [0, 1] is the intersection of the three curves $\Delta_0 = 0$, $\Delta_1 = 0$, and one branch of $\Delta_3 = 0$. Point A with coordinates $[0, 1/(1-e^2)]$ is the self-intersection of curve $\Delta_2 = 0$, as well as the intersection of one branch of $\Delta_3 = 0$ with $\Delta_2 = 0$. Point C with coordinates $[2e(9-4e^2)^{-0.5}, 1 - e^2(1-e^2)^{-0.5}(9-4e^2)^{-0.5}]$ is the intersection of the three curves $\Delta_1 = 0$, one branch of $\Delta_2 = 0$, and one branch of $\Delta_3 = 0$. The whole figure is symmetrical across axis $k_1 = 0$. By analyzing conditions (22) and (23), we conclude that the projected curve of the relative orbit does not self-intersect if the parameters are in the white area; it self-intersects once in the lightly shaded area, and self-intersects twice in the darkly shaded area. Points 1, 2, 3, and 4 are sample points of an example given at the end of this section.

C. Projection onto the In-Track/Cross-Track Plane

When the relative orbit projected onto the in-track/cross-track plane self-intersects, Eqs. (15–17) are satisfied. Expressing m with n through Eq. (16), substituting the consequent expression into Eqs. (15) and (17) using Eqs. (19), we obtain

$$\begin{cases} (1-e)^2\{(1-k_1k_3)[(1+e)+(1-e)k_3^2] - [(1+e)k_2 + k_1k_3](1+k_3^2)\}m^2 + 2e(1-e)[(1+e)k_1 + (3-e)k_1k_3^2 + 2(1+e)k_2k_3]m \\ \quad - 4e^2[(1+e)k_2 + k_1k_3] = 0 \\ m^2 + 4k_3 m - 4\frac{1+e}{1-e} > 0 \end{cases} \tag{24}$$

Analogously, the discriminants Δ_0, Δ_1, Δ_2, and Δ_3 for the y–z plane are given as Eqs. (A12–A15) in the Appendix. The conditions for the projected curve with a different number of self-intersection points are the same as in Sec. III.B. However, as shown in the Appendix, the discriminants are too complex to be represented in simple graphs. We nevertheless give an example with four cases in Table 1 to substantiate the conclusions.

D. Example 1

After dividing the x and y components by c_2, and the z component by c_4, we substitute the parameters in Table 1 into Eqs. (7) to obtain the dimensionless relative orbits projected onto the coordinate planes as shown in Fig. 4. These projected curves self-intersect according to the number of times predicted in Table 1. Note that the last subfigure of Fig. 4 does self-intersect twice, despite the blurry appearance caused by the scale limit.

IV. Three-Dimensional Relative Orbit Geometry

To Eqs. (1) we now apply the widely known equations for Keplerian elliptical motion, $r = a(1-e^2)/(1+e\cos f)$ and $\theta = \omega + f$. In addition to the constant orbit elements, the precise relative position is shown to be governed by two time-dependent arguments, the true anomaly of the leader f and that of the follower f_f. If we neglect their dependence on time, treating them instead as time-independent variables, Eqs. (1) constitute the parametric equations of a closed surface. An analogous treatment can be found in [26] with greater details, in which the general solutions to the relative motion are the same in essence as the precise equations of relative position, Eqs. (1) here, although they differ in form. However, the main focus of this paper is not the precise equations, but the first-order approximation ones, Eqs. (2), and their algebraic equivalence, Eqs. (7).

A. Dimensionality of the Relative Orbit

One of our primary interests in the relative orbit is whether it is planar or spatial, and if the former, how to determine its plane. In theory, with the parametric equations of the relative orbit known, its curvature and torsion can be calculated with the application of differential geometry, and its dimensionality and topology (including self-intersecting attributes) obtained. In practice, however, considerable complexity is involved. Let us assume that the relative orbit expressed by Eqs. (7) is on the plane $n_1x + y + n_3z = n_0$, where $(n_1, 1, n_3)^T$ denotes the x, y, and z components of the normal vector of the plane, respectfully, normalized for the y component. The normalization can be carried out because if the normal vector in the y component is zero, the particular case $n_1x + n_3z = n_0$ applied to Eqs. (7) implies 1) $c_1 = c_2 = 0$, and $c_4 = c_5 = 0$ for $e \neq 0$, or 2) $c_4 = 0$, $n_1/n_3 = c_5/c_1$, and $n_0 = 0$ for $e = 0$. This degenerate case is excluded from our interest. Then, substituting Eqs. (7) into the preceding plane equation, after combining the coefficients, we obtain

$$\frac{(ec_2n_1 + c_1)s + ec_2 - c_1n_1}{s^2+1} + \frac{(c_4n_3 + c_1)s + c_5n_3 - ec_3}{(1-e)s^2 + 1 + e} = \frac{1}{2}[n_0 - c_1n_1 - (1-e)c_2 - c_3 + c_5n_3] \tag{25}$$

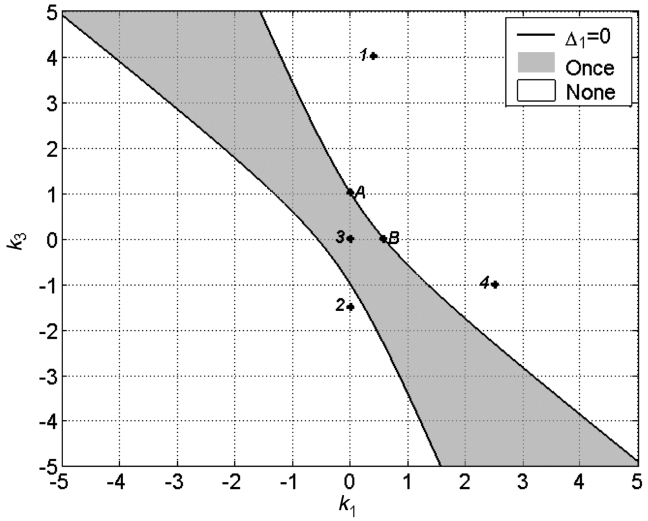

Fig. 2 Self-intersection discriminance on the radial/cross-track plane.

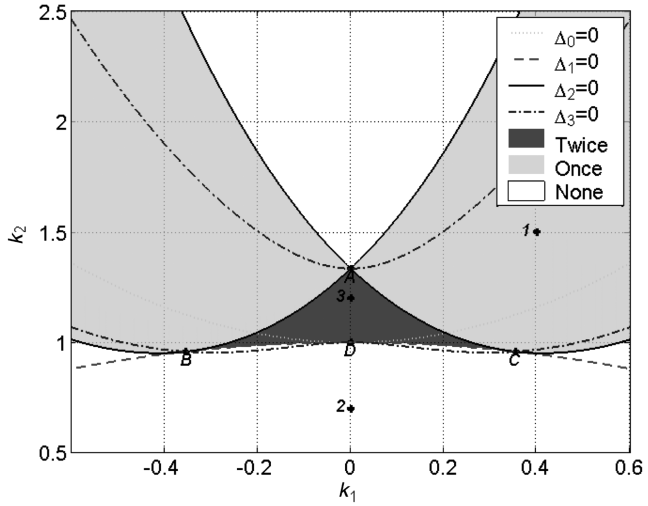

Fig. 3 Self-intersection discriminance on the radial/in-track plane.

which holds for any arbitrary s. When $e = 0$ and $c_4 \neq 0$, it is easy to determine the normal vector of the plane:

$$n_1 = -2c_5/c_4, \qquad n_3 = -2c_1/c_4, \qquad n_0 = c_2 + c_3 \tag{26}$$

On the other hand, when $e \neq 0$, there exists no nonzero constant n_1 and n_3 so that Eq. (25) holds for any arbitrary s. That is to say, in a circular reference orbit, the relative orbit is always planar, whereas in an elliptical reference orbit, the orbit is generally three-dimensional except for the degenerate cases when $c_1 = c_2 = 0$ or $c_4 = c_5 = 0$.

B. Collision Between the Follower and the Leader

One practical issue to be considered in formation flying is whether the follower will collide with the leader. Formulated mathematically, a collision occurs when the relative orbit written as Eqs. (7) passes through the origin. We therefore examine the condition for $(0, 0, 0)$ to be a solution to Eqs. (7). For $x = 0$, Eqs. (7) yield

$$s^2 = 1 - 2ec_2 s/c_1 \tag{27}$$

Similarly, $z = 0$ gives

$$s^2 = 1 + 2c_4 s/[(1-e)c_5] \tag{28}$$

Equations (27) and (28) have at least one common real solution of s if and only if

$$c_1 c_4 + e(1-e)c_2 c_5 = 0 \tag{29}$$

Lastly, with $y = 0$ in Eqs. (7), we obtain a fractional equation. Multiplying this equation by $(s^2+1)[(1-e)s^2 + 1 + e]$, and substituting Eq. (27) for all the quadratic terms of s, we simplify this equation into the form $As = B$, where A and B are expressions with respect to e, c_1, c_2, and c_3. Substituting $s = B/A$ into Eq. (27), we arrive at

$$4c_1^2 - (1-e)[(1-e)c_2 + c_3][(1+e)^2 c_2 + (1-e)c_3] = 0 \tag{30}$$

Equations (29) and (30) combine to represent the conditions for collision between the follower and the leader. For a verification, consider the case of $c_1 = 0$. The collision conditions lead to two nondegenerate (none of the x, y, and z components vanish) cases: 1) $c_5 = 0$, and $c_3 = -(1-e)c_2$, or 2) $c_5 = 0$, and $c_3 = -(1+e)^2 c_2/(1-e)$. Substitution of these two conditions into Eqs. (7) yields $x = y = z = 0$ at $s = \infty$ in case 1 and $s = 0$ in case 2. The reason for choosing $c_1 = 0$ as an example is that Eqs. (27) and (28) have singularity at these values which may make results unreliable. It is worth noting that these conditions are derived from the FRPE which entails second-order error. Consequently, even if the collision conditions are satisfied mathematically, the collision may not necessarily occur in reality. Nevertheless, confining the relative distance between the follower and the leader to a second-order value is beneficial to spacecraft docking as well as collision avoidance in formation designs.

C. Spatial Self-Intersection of Relative Orbit

In Sec. III, we discussed the self-intersection of the relative orbit projected onto the coordinate planes. Moreover, the relative orbit may self-intersect spatially, namely Eqs. (14–17) are all satisfied. This implies

$$\begin{cases} m = \frac{2e^2 c_2 c_4}{(1-e)(ec_2 c_5 + c_1 c_4)} \\ n = \frac{e(1-e)c_2 c_5 + (1+e)c_1 c_4}{(1-e)(ec_2 c_5 + c_1 c_4)} \end{cases} \tag{31}$$

$$ec_2[(1+e)c_4^2 + (1-e)c_5^2] - c_4(ec_3 c_4 + c_1 c_5) = 0 \tag{32}$$

$$\begin{aligned} \Delta &= m^2 - 4n \\ &= \frac{4[e^4 c_2^2 c_4^2 - e^2(1-e)^2 c_2^2 c_5^2 - (1-e^2)c_1^2 c_4^2 - 2e(1-e)c_1 c_2 c_4 c_5]}{(1-e)^2(ec_2 c_5 + c_1 c_4)^2} \\ &> 0 \end{aligned} \tag{33}$$

Table 1 Parameters selected for self-intersection

Case	1	2	3	4
	$k_1 = 0.4, k_2 = 1.5, k_3 = 4$	$k_1 = 0, k_2 = 0.7, k_3 = -1.5$	$k_1 = 0, k_2 = 1.2, k_3 = 0$	$k_1 = 2.5, k_2 = 4, k_3 = -1$
x–z plane	$\Delta_1 > 0$ does not self-intersect	$\Delta_1 > 0$ does not self-intersect	$\Delta_1 < 0$ self-intersects once	$\Delta_1 > 0$ does not self-intersect
x–y plane	$\Delta_1 > 0, \Delta_2 < 0$ self-intersects once	$\Delta_1 < 0$ does not self-intersect	$\Delta_1 > 0, \Delta_2 > 0, \Delta_3 > 0$ self-intersects twice	$\Delta_0 \neq 0, \Delta_1 > 0, \Delta_2 > 0, \Delta_3 < 0$ does not self-intersect
y–z plane	$\Delta_0 \neq 0, \Delta_1 > 0, \Delta_2 > 0, \Delta_3 < 0$ does not self-intersect	$\Delta_1 > 0, \Delta_2 < 0$ self-intersects once	$\Delta_1 < 0$ does not self-intersect	$\Delta_1 > 0, \Delta_2 > 0, \Delta_3 > 0$ self-intersects twice

Equations (32) and (33) are the conditions of self-intersection. The solutions of s, denoted by $s_{1,2}$, as well as the coordinates of the self-intersection point, denoted by (x^*, y^*, z^*), can be derived from Eqs. (7) and (31) as follows:

$$\begin{cases} x^* = \frac{e(1-e)c_2c_5+c_1c_4}{ec_4} \\ y^* = \frac{2c_4(c_1^2+e^2c_2^2)-c_1[e(1-e)c_2c_5+c_1c_4]}{e^2c_2c_4} \\ z^* = \frac{e(1-e)c_2c_5+c_1c_4}{e^2c_2} \end{cases} \tag{34}$$

$$s_{1,2}^* = \frac{e^2c_2c_4 \pm \sqrt{e^4c_2^2c_4^2 - e^2(1-e)^2c_2^2c_5^2 - (1-e^2)c_1^2c_4^2 - 2e(1-e)c_1c_2c_4c_5}}{(1-e)(ec_2c_5 + c_1c_4)} \tag{35}$$

To sum up, the real or imaginary self-intersection will occur in a relative orbit when the parameters $c_j (j = 1, 2, \ldots, 5)$ satisfy Eq. (32). In particular, if these parameters satisfy inequality (33), the self-intersection is real; otherwise, it is imaginary because of the imaginary value of s. The coordinates of the only self-intersection point are given by Eqs. (34), and the value of s at this point is given by Eq. (35). By combining the preceding conclusions with Eq. (6), the value of f can also be determined.

Let us examine some special self-intersection points using the preceding conclusions. Setting $x^* = y^* = z^* = 0$ in Eqs. (34), we find that there are no nonsingular solutions to the parameters $c_j (j = 1, 2, \ldots, 5)$. That is to say, the relative orbit cannot pass through the origin, which is the position of the leader spacecraft, more than once, unless the orbits of the follower and leader spacecraft are identical. If $x^* = z^* = 0$ and $y^* \neq 0$, we can obtain $c_4 = -e(1-e)c_2c_5/c_1$ and $y^* = 2[(c_1)^2 + (ec_2)^2]/(e^2c_2)$. Substitution for c_4 in Eq. (32) yields $c_3 = [2(c_1)^2 + (1-e^2)(ec_2)^2]/[e^2(1-e)c_2]$. It is not difficult to prove that such c_4 satisfies the inequality (33). Therefore, one is able to design a formation so that the relative orbit passes through a point in the in-track direction twice.

D. Relative Orbit on a Quadric Surface

In Sec. IV.A, we conclude that for arbitrary elliptical reference orbits, it is not possible for the relative orbit to be planar except in particular degenerate cases. Gurfil and Kholshevnikov [26] stated that when some of the relative orbit elements are of first-order small values, the relative orbit is on an elliptic torus, which is a quartic surface. In this section, we discuss the finding that the relative orbit is always on a certain quadric surface. Because the orbit is not on any plane, as a try, we assume that there exist coefficients $\{a_{11}, a_{22}, a_{33}, a_{12}, a_{23}, a_{13}, a_1, a_2, a_3, a_0\}$ such that

$$\begin{aligned} &a_{11}x^2 + a_{22}y^2 + a_{33}z^2 + 2a_{12}xy + 2a_{23}yz + 2a_{13}xz \\ &\quad + 2a_1x + 2a_2y + 2a_3z + a_0 = 0 \end{aligned} \tag{36}$$

where x, y, and z are given by Eqs. (7). With some effort, these coefficients can be deduced as follows:

$$\begin{cases} a_{11} = a_{22} = (1+e)c_4^2 + (1-e)c_5^2 \\ a_{33} = (1+e)c_1^2 + e^2(1-e)c_3^2 \\ a_{23} = -[(1+e)c_1c_4 - e(1-e)c_3c_5] \\ a_{13} = -(c_1c_5 + ec_3c_4), \quad a_{12} = 0, \quad a_1 = 0 \\ a_2 = \frac{1-e}{e}c_5[(1+e)c_1c_4 - e(1-e)c_3c_5] - c_2[(1+e)c_4^2 + (1-e)c_5^2] - \frac{c_4}{e}(c_1c_5 + ec_3c_4) \\ a_3 = [c_2 + (1-e)c_3][(1+e)c_1c_4 - e(1-e)c_3c_5] + 2ec_1(c_1c_5 + ec_3c_4) \\ a_0 = 4(c_1c_5 + ec_3c_4)[ec_2c_4 - (1-e)c_1c_5] - \frac{1}{1+e}[e(1-e)c_3c_5 - (1+e)c_1c_4]^2 + \frac{1-e}{1+e}[(1+e)c_2 + c_3]^2[(1+e)c_4^2 + (1-e)c_5^2] \end{cases} \tag{37}$$

Because these coefficients satisfy Eq. (36) no matter how the variable s varies, it can be stated that the relative orbit expressed by Eqs. (7) is always on a certain quadric surface.

The mathematical theory of quadric surfaces identifies four invariants that are unaffected by coordinate transformations. To determine the type of quadric surface the relative orbit is on, we evaluate the four invariants of the quadric surface in Eq. (36), I_{1-4}. This and subsequent applications of the theory of quadric surfaces can also be found in [27].

$$\begin{aligned} I_1 &= a_{11} + a_{22} + a_{33} = 2[(1+e)c_4^2 + (1-e)c_5^2] \\ &\quad + (1+e)c_1^2 + e^2(1-e)c_3^2 > 0 \end{aligned} \tag{38}$$

$$\begin{aligned} I_2 &= \begin{vmatrix} a_{11} & a_{12} \\ a_{12} & a_{22} \end{vmatrix} + \begin{vmatrix} a_{22} & a_{23} \\ a_{23} & a_{33} \end{vmatrix} + \begin{vmatrix} a_{33} & a_{13} \\ a_{13} & a_{11} \end{vmatrix} \\ &= [(1+e)c_4^2 + (1-e)c_5^2]^2 + [e(1-e)c_3c_5 - (1+e)c_1c_4]^2 \\ &\quad + (1-2e^2)(c_1c_5 + ec_3c_4)^2 \end{aligned} \tag{39}$$

$$\begin{aligned} I_3 &= \begin{vmatrix} a_{11} & a_{12} & a_{13} \\ a_{12} & a_{22} & a_{23} \\ a_{13} & a_{23} & a_{33} \end{vmatrix} = -e^2[(1+e)c_4^2 \\ &\quad + (1-e)c_5^2](c_1c_5 + ec_3c_4)^2 \le 0 \end{aligned} \tag{40}$$

$$\begin{aligned} I_4 &= \begin{vmatrix} a_{11} & a_{12} & a_{13} & a_1 \\ a_{12} & a_{22} & a_{23} & a_2 \\ a_{13} & a_{23} & a_{33} & a_3 \\ a_1 & a_2 & a_3 & a_0 \end{vmatrix} = e^2\{ec_2[(1+e)c_4^2 + (1-e)c_5^2] \\ &\quad - c_4(c_1c_5 + ec_3c_4)\}^2(c_1c_5 + ec_3c_4)^2 \ge 0 \end{aligned} \tag{41}$$

The invariant I_1 is greater than zero because the degenerate case $c_4 = c_5 = 0$ is not considered. The center of the quadric surface, of which the coordinates are denoted by (x_0, y_0, z_0), is decided by

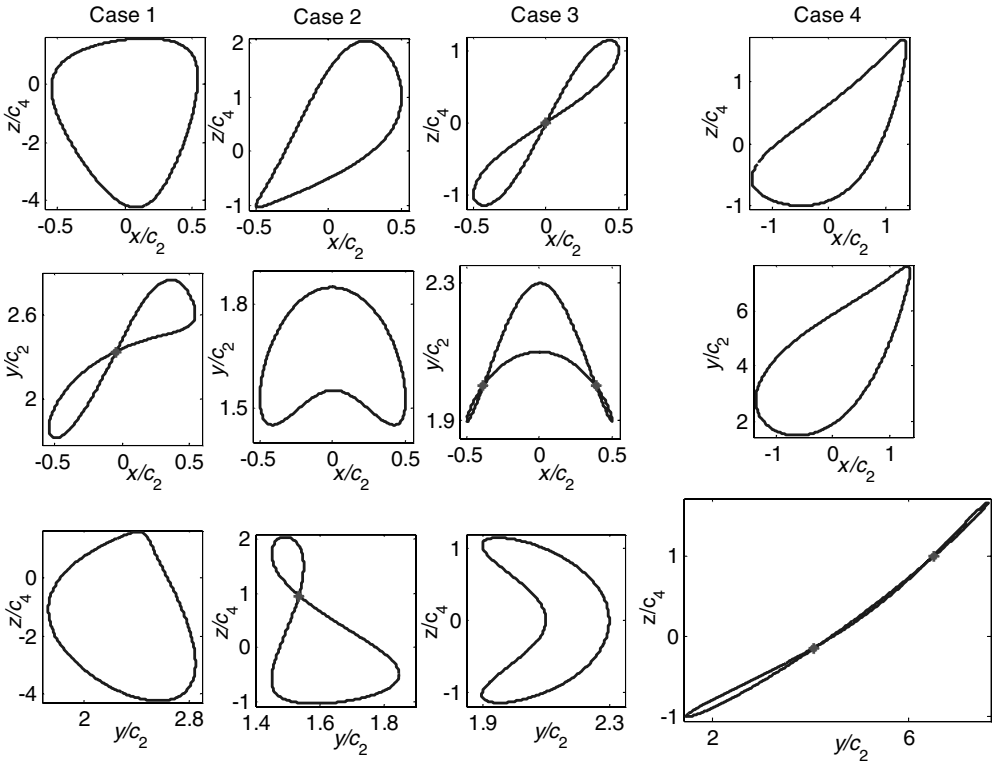

Fig. 4 Relative orbits projected onto the coordinate planes.

$$\begin{cases} a_{11}x_0 + a_{12}y_0 + a_{13}z_0 + a_1 = 0 \\ a_{12}x_0 + a_{22}y_0 + a_{23}z_0 + a_2 = 0 \\ a_{13}x_0 + a_{23}y_0 + a_{33}z_0 + a_3 = 0 \end{cases} \tag{42}$$

whose solutions are

$$\begin{cases} x_0 = \frac{c_1}{e} + \frac{(1-e)c_5(c_1c_5+ec_3c_4)}{e[(1+e)c_4^2+(1-e)c_5^2]} \\ y_0 = c_2 - (1-e)c_3 + \frac{c_4\{(2-e^2)(c_1c_5+ec_3c_4)^2+[(1+e)c_1c_4-e(1-e)c_3c_5]^2\}}{e[(1+e)c_4^2+(1-e)c_5^2](c_1c_5+ec_3c_4)} \\ z_0 = \frac{1-e}{e}c_5 + \frac{c_1[(1+e)c_4^2+(1-e)c_5^2]}{e(c_1c_5+ec_3c_4)} \end{cases} \tag{43}$$

Meanwhile, its characteristic equation

$$\begin{vmatrix} a_{11}-u & a_{12} & a_{13} \\ a_{12} & a_{22}-u & a_{23} \\ a_{13} & a_{23} & a_{33}-u \end{vmatrix} = 0 \tag{44}$$

gives the three eigenvalues

$$\begin{cases} u_1 = a_{11} = (1+e)c_4^2 + (1-e)c_5^2 > 0 \\ u_2 = \frac{1}{2}[a_{11}+a_{33}+\sqrt{(a_{11}+a_{33})^2+4e^2a_{13}^2}] > 0 \\ u_3 = \frac{1}{2}[a_{11}+a_{33}-\sqrt{(a_{11}+a_{33})^2+4e^2a_{13}^2}] \le 0 \end{cases} \tag{45}$$

where the relationship $a_{23}^2 - a_{11}a_{33} = -(1-e^2)a_{13}^2$, derived from Eqs. (37), is used. The corresponding three normalized eigenvectors are derived from Eq. (44) as

$$\begin{cases} X_1 = \frac{1}{\sqrt{a_{13}^2+a_{23}^2}}[a_{23}, -a_{13}, 0]^T \\ X_2 = \frac{1}{\sqrt{(u_2-a_{11})^2+a_{13}^2+a_{23}^2}}[a_{13}, a_{23}, u_2-a_{11}]^T \\ X_3 = \frac{1}{\sqrt{(u_3-a_{11})^2+a_{13}^2+a_{23}^2}}[a_{13}, a_{23}, u_3-a_{11}]^T \end{cases} \tag{46}$$

The principal axis frame of the quadric surface is denoted as $\tilde{L}\,\tilde{x}\,\tilde{y}\,\tilde{z}$, of which the coordinates of the origin $\tilde{L}$ in the frame $Lxyz$ are (x_0, y_0, z_0). The transforming matrix $A_{\tilde{L}L}$, which transforms any vector in the frame $Lxyz$ into the frame $\tilde{L}\,\tilde{x}\,\tilde{y}\,\tilde{z}$, is formed by the eigenvectors as

$$A_{\tilde{L}L} = [X_1, X_2, X_3]^T \tag{47}$$

The quadric surface, written as Eq. (36) in the old frame, can be written in the new frame as

$$u_1\tilde{x} + u_2\tilde{y} + u_3\tilde{z} + I_4/I_3 = 0 \tag{48}$$

where I_3 is nonzero.

1. One-Sheet Hyperboloid

If $I_3I_4 \neq 0$, it can be concluded that $I_3 < 0$, $I_4 > 0$, and $c_1c_5 + ec_3c_4 \neq 0$, as shown in Eqs. (40) and (41). Moreover, we can obtain that $a_{13} \neq 0$, and accordingly $u_3 < 0$. Hence, Eq. (48) can be rebuilt as

$$\frac{\tilde{x}^2}{-I_4/(u_1I_3)} + \frac{\tilde{y}^2}{-I_4/(u_2I_3)} - \frac{\tilde{z}^2}{I_4/(u_3I_3)} = 1 \tag{49}$$

which is known as the canonical equation of a one-sheet hyperboloid. That is to say, if

$$\begin{cases} ec_2[(1+e)c_4^2 + (1-e)c_5^2] - c_4(c_1c_5 + ec_3c_4) \neq 0 \\ c_1c_5 + ec_3c_4 \neq 0 \end{cases} \tag{50}$$

the relative orbit is always on a hyperboloid of one sheet; its equation in the principal axis frame is given by Eq. (49), the center coordinates in the frame $Lxyz$ are given by Eqs. (43), and the transforming matrix is given by Eq. (47).

2. Elliptic Cone

If $I_3 \neq 0$ and $I_4 = 0$, namely

$$\begin{cases} ec_2[(1+e)c_4^2 + (1-e)c_5^2] - c_4(c_1c_5 + ec_3c_4) = 0 \\ c_1c_5 + ec_3c_4 \neq 0 \end{cases} \tag{51}$$

Equation (48) can be rebuilt as

$$\frac{\tilde{x}^2}{1/u_1}+\frac{\tilde{y}^2}{1/u_2}-\frac{\tilde{z}^2}{-1/u_3}=0 \tag{52}$$

which is known as the canonical equation of an elliptic cone. From Eq. (51), we can derive c_3 in terms of other parameters. Substitution of the consequent expression of c_3 into Eqs. (43) results in the center coordinates identical to the coordinates of the self-intersection point as shown by Eqs. (34) in Sec. IV.C. It behooves us to question the relationship between the elliptic cone conditions (51) and the real self-intersection conditions (32) and (33). A simple analysis reveals that the latter is a subset of the former. If $c_1c_5+ec_3c_4=0$, $c_2=0$ can be deduced from the conditions (51). Conversely, the two relations do not satisfy condition (33), and when substituted into Eqs. (34) and (35) give the coordinates of the self-intersection point as $(c_1/e,\infty,\infty)$ with an imaginary value of s. To sum up, the relative orbit must be on an elliptic cone if it has a self-intersection point, either real or imaginary, so long as it is not at infinity.

3. Elliptic Cylinder

If $I_3=0$, $I_4=0$, and $I_2\neq 0$, namely

$$c_1c_5+ec_3c_4=0 \tag{53}$$

then $a_{13}=0$, and the eigenvalue $u_3=0$. To describe the quadric surface, it is necessary to introduce the semi-invariant K_2, defined as follows:

$$K_2=\begin{vmatrix} a_{11} & a_{12} & a_1\\ a_{12} & a_{22} & a_2\\ a_1 & a_2 & a_0\end{vmatrix}+\begin{vmatrix} a_{11} & a_{13} & a_1\\ a_{13} & a_{33} & a_3\\ a_1 & a_3 & a_0\end{vmatrix}+\begin{vmatrix} a_{22} & a_{23} & a_2\\ a_{23} & a_{33} & a_3\\ a_2 & a_3 & a_0\end{vmatrix} \tag{54}$$

The quadric surface expressed by Eq. (36) degenerates into

$$u_1\tilde{x}^2+u_2\tilde{y}^2+K_2/I_2=0 \tag{55}$$

Two subcases follow:

Case 3.1: If $c_5\neq 0$, Eq. (53) leads to $c_1=-ec_3c_4/c_5$. Then Eq. (54) gives

$$K_2=-\frac{e^2}{c_5^4}(c_2^2c_5^2+c_3^2c_4^2)[(1+e)c_4^2+(1-e)c_5^2]^3[e^2c_3^2+c_5^2] \tag{56}$$

The second invariant I_2 becomes

$$I_2=\frac{1}{c_5^2}[(1+e)c_4^2+(1-e)c_5^2]^2[e^2c_3^2+c_5^2] \tag{57}$$

Equation (55) is reduced to

$$c_5^2\tilde{x}^2+(e^2c_3^2+c_5^2)\tilde{y}^2=e^2(c_2^2c_5^2+c_3^2c_4^2) \tag{58}$$

which represents an elliptic cylinder. There exists an infinite set of centers for elliptic cylinders, among which we specify a representative center with the coordinates

$$(x_0,y_0,z_0)=(0,c_2+c_3-ec_3,0) \tag{59}$$

Consequently, the transforming matrix can be written as

$$A_{\tilde{L}L}=\frac{1}{\sqrt{e^2c_3^2+c_5^2}}\begin{bmatrix}\sqrt{e^2c_3^2+c_5^2} & 0 & 0\\ 0 & c_5 & ec_3\\ 0 & -ec_3 & c_5\end{bmatrix} \tag{60}$$

Case 3.2: If $c_5=0$, then $c_4\neq 0$ because the degenerate relative motion is excluded. Therefore, Eq. (53) leads to $c_3=0$. Similarly, the quadric surface degenerates into

$$c_4^2\tilde{x}^2+(c_1^2+c_4^2)\tilde{y}^2=c_4^2(c_1^2+e^2c_2^2) \tag{61}$$

which likewise represents an elliptic cylinder with its representative center coordinates specified as

$$(x_0,y_0,z_0)=(0,c_2,0) \tag{62}$$

and the consequent transforming matrix is

$$A_{\tilde{L}L}=\frac{1}{\sqrt{c_1^2+c_4^2}}\begin{bmatrix}\sqrt{c_1^2+c_4^2} & 0 & 0\\ 0 & c_4 & -c_1\\ 0 & c_1 & c_4\end{bmatrix} \tag{63}$$

Under the condition of Eq. (53), a simple analysis shows that if $c_2=0$, the relative orbit has an imaginary self-intersection point at infinity; otherwise, the relative orbit has no self-intersection point. So long as the condition of Eq. (53) is satisfied, allowing a self-intersection point at infinity, the relative orbit must be on an elliptic cylinder.

E. Example 2

Let us choose the orbit elements of the leader $[a,e,i,\Omega,M_0,\omega]=[1.4\times10^4\text{ km},0.5,\pi/3\text{ rad},0,\pi/4\text{ rad},\pi/6\text{ rad}]$, and five sets of parameters $c_j(j=1,2,\ldots,5)$ as shown in Table 2, so that the corresponding relative orbits are, respectively, on a one-sheet hyperboloid, an elliptic cone with real self-intersection, an elliptic cone with imaginary self-intersection, an elliptic cylinder with $c_5\neq 0$, and an elliptic cylinder with $c_5=0$. By Eqs. (4), the corresponding orbit element differences can be evaluated as shown in Table 2.

Cases 1, 2.1, 2.2, 3.1, and 3.2 are depicted by Figs. 5–9, respectively. In each figure, the dash-dotted line represents the accurate relative orbit obtained through Eqs. (1), the solid line represents the first-order relative orbit obtained through Eqs. (2), and the shaded surface represents the quadric surface on which the relative orbit rests. Note that the metrics used to generate the quadric surface, such as canonical equations, center coordinates, and transforming matrixes, are different for the one-sheet hyperboloid, elliptic cone, and elliptic cylinder with c_5 equal and unequal to zero, as previously discussed. Because the error between the first-order relative orbit and the accurate orbit is of the second-order, the dash-dotted line appears to overlap with the solid line in each figure. The relative orbit in each case is on the expected quadric surface as specified in the preceding analysis.

In a peculiar case, in which $I_3=0$, $I_4=0$, and $I_2=0$, the result $c_4=c_5=0$, corresponding to the degenerate case, was excluded from our interest. In conclusion, for any nondegenerate relative motion, the relative orbit must be on one of the three types of quadric surfaces: most frequently, a one-sheet hyperboloid; in some particular cases, an elliptic cone or an elliptic cylinder.

Table 2 Parameters selected for relative orbits on quadric surfaces

Case	$[c_1,c_2,c_3,c_4,c_5]$, km	$[\Delta e,\Delta i,\Delta\Omega,\Delta M,\Delta\omega]$, $\times10^{-3}$	Quadric surface
1	[12.5, 10, 60, 10, −10]	[0.893, 0.587 rad, 1.026 rad, 0.619 rad, 2.344 rad]	one-sheet hyperboloid
2.1	[10, −20, −60, 10, 10]	[0.714, 1.063 rad, 0.0737 rad, −1.237 rad, −2.894 rad]	elliptic cone
2.2	[10, 20, 20, 10, 10]	[0.714, 1.063 rad, 0.0737 rad, 1.237 rad, 0.916 rad]	elliptic cone
3.1	[10, 20, −20, 10, 10]	[0.714, 1.063 rad, 0.0737 rad, 1.237 rad, −0.989 rad]	elliptic cylinder
3.2	[20, 10, 0, −10, 0]	[1.429, −0.825 rad, −0.550 rad, 0.619 rad, 0.275 rad]	elliptic cylinder

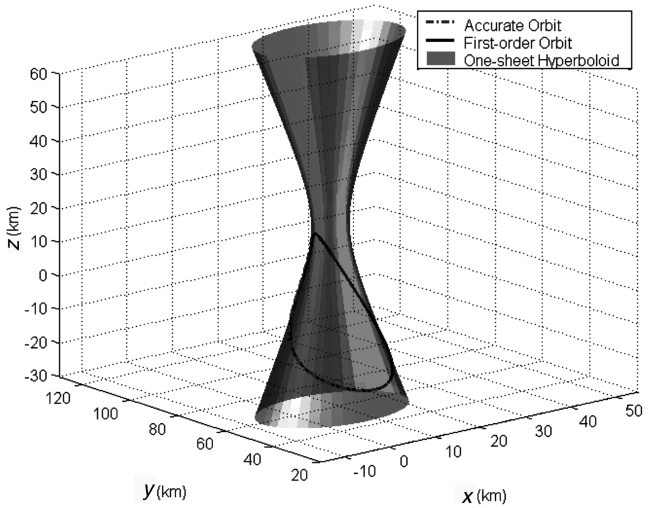

Fig. 5 Relative orbit on a one-sheet hyperboloid.

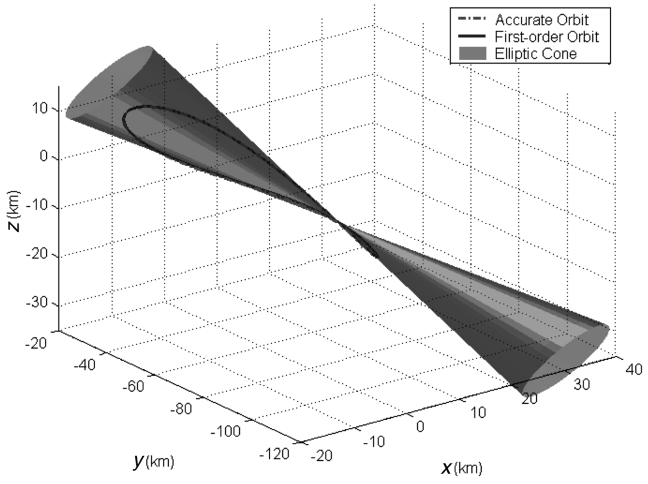

Fig. 6 Self-intersecting relative orbit on an elliptic cone.

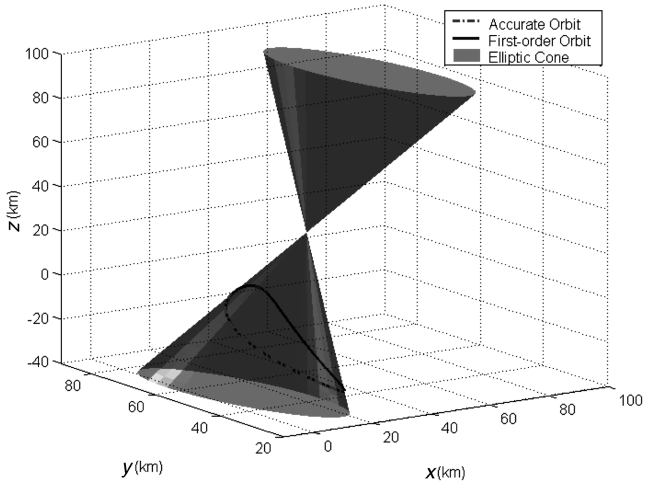

Fig. 7 Relative orbit on an elliptic cone.

V. Conclusions

Based on the first-order relative position equations which model the relative motion of unperturbed spacecraft formation with the reference orbital element approach, a set of algebraic equations have been derived through parametric transformations. These algebraic equations prove to be applicable to the periodic solutions of the widely cited Lawden's equations. With algebraic methods, some interesting characters of the relative orbit geometry in spacecraft formations flying are deduced. Under the condition of equal semimajor axes without perturbations, the projections of the relative orbit onto the three coordinate planes of the leader local-vertical–local-horizontal frame are all closed curves.

First, we conclude that the relative orbit projected onto the radial/cross-track plane may self-intersect at most once, and the relative orbit projected either onto the radial/in-track plane or onto the in-track/cross-track plane may self-intersect at most twice. The corresponding discriminants determining the number of self-intersections for each projected curve are obtained in terms of the parameters of the algebraic equations. These parameters can be readily transformed into orbit element differences if necessary.

Second, we conclude that for an elliptical reference orbit, the relative orbit is generally a nonplanar curve in the three-dimensional space, except in the degenerate case where the relative motion in the radial, in-track, or cross-track direction vanishes. In the examination of the spatial curve, the conditions of collision between the follower and the leader are obtained, which can be used for spacecraft docking and collision avoidance. The conditions for the relative orbit to self-intersect spatially are also determined. An interesting characteristic of the relative orbit geometry is that the relative orbit always rests on one of the three types of quadric surfaces. Generally, the relative orbit is on a certain one-sheet hyperboloid. In the particular case in which the relative orbit has a real or finite imaginary self-intersection point,

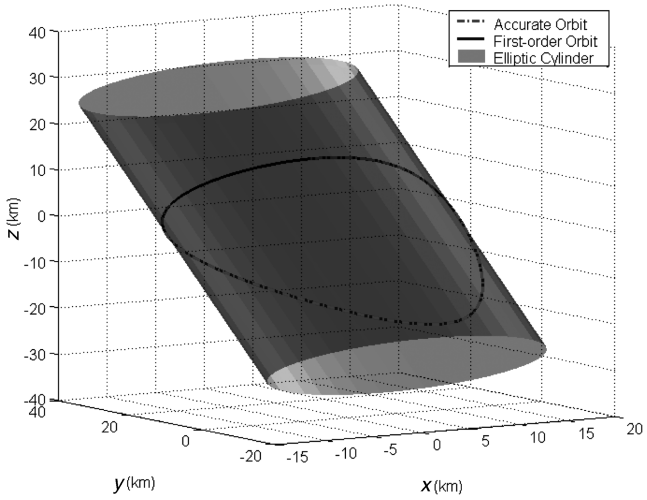

Fig. 8 Relative orbit on an elliptic cylinder ($c_5 \neq 0$).

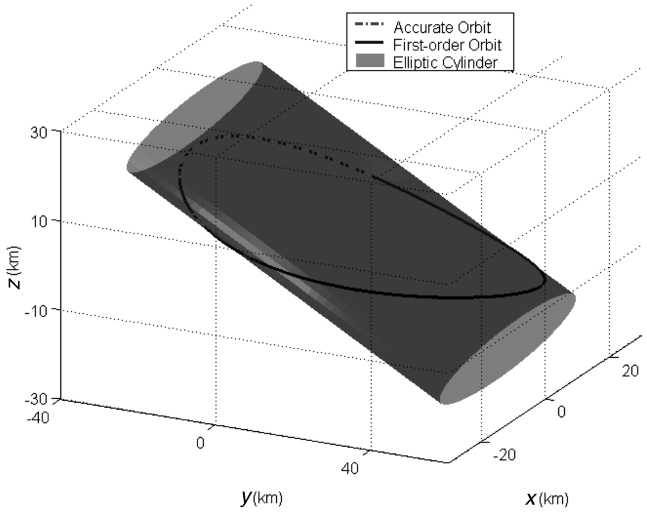

Fig. 9 Relative orbit on an elliptic cylinder ($c_5 = 0$).

the relative orbit is on an elliptic cone. In the rest of the cases, including the one with an imaginary self-intersection point at infinity, the relative orbit is on an elliptic cylinder. For nondegenerate relative motion, these three types of quadric surfaces exhaust the possibilities of the relative orbit geometry, and their corresponding discriminants are presented.

Appendix: Solution to Quadratic Combined Equations Including Inequality

Equations (21) and (24) can be generalized as the following combined equations:

$$\begin{cases} \lambda_0 x^2 + \lambda_1 x + \lambda_2 = 0 \\ x^2 + \lambda_3 x + \lambda_4 > 0 \end{cases} \tag{A1}$$

where $\lambda_j (j = 0, 1, \ldots, 4)$ are coefficients. There exists, at most, two solutions with respect to x, and possibly one or none, depending on the coefficients. The discriminant of the quadratic equation in Eqs. (A1) is

$$\Delta_a = \lambda_1^2 - 4\lambda_2\lambda_0 \tag{A2}$$

which, when no less than zero, guarantees the real solutions

$$x = (-\lambda_1 \pm \sqrt{\lambda_1^2 - 4\lambda_2\lambda_0})/(2\lambda_0) \tag{A3}$$

Substitution of the solutions into the inequality in Eqs. (A1) results in the following inequalities, denoted by $\Delta_\pm$:

$$\Delta_\pm = \lambda_1(\lambda_1 - \lambda_3\lambda_0) + 2\lambda_0(\lambda_4\lambda_0 - \lambda_2) \pm (\lambda_1 - \lambda_3\lambda_0)\sqrt{\lambda_1^2 - 4\lambda_2\lambda_0} > 0 \tag{A4}$$

Then there exists two real solutions for Eqs. (A1) if

$$(\Delta_a > 0) \cap (\Delta_+\Delta_- > 0) \cap (\Delta_+ + \Delta_- > 0) \tag{A5}$$

where the first inequality guarantees that there are two distinct real solutions for the quadratic equation, and the last two inequalities ensure that Δ_+ and Δ_- both have the same positive sign so as to satisfy the inequalities in Eqs. (A4). The existence conditions in Eqs. (A5) for two real solutions to Eqs. (A1) can be translated into the conditions for the coefficients:

$$\begin{cases} \Delta_a = \lambda_1^2 - 4\lambda_2\lambda_0 > 0 \\ \Delta_+\Delta_- = (\lambda_1 - \lambda_3\lambda_0)(\lambda_1\lambda_4 - \lambda_2\lambda_3) + (\lambda_4\lambda_0 - \lambda_2)^2 > 0 \\ \Delta_+ + \Delta_- = \lambda_1(\lambda_1 - \lambda_3\lambda_0) + 2\lambda_0(\lambda_4\lambda_0 - \lambda_2) > 0 \end{cases} \tag{A6}$$

It can be asserted that there is no real solution to Eqs. (A1) if

$$[(\lambda_0 \neq 0) \cap (\Delta_a \geq 0) \cap (\Delta_+\Delta_- \geq 0) \cap (\Delta_+ + \Delta_- \leq 0)] \cup [\Delta_a < 0] \tag{A7}$$

where the conditions in the first pair of square brackets guarantee that there is at least one real solution to the quadratic equation in Eqs. (A1), but none to inequalities in Eqs. (A4), and the condition in the last pair of square brackets implies that there is no real solution to the quadratic equation in Eqs. (A1). Note that to accord with Eqs. (21) and (24), which allow the infinite solution to m, here $\lambda_0 = 0$ is excluded from conditions (A7) because it will result in the solution $x = \infty$ to Eqs. (A1). The nonexistence conditions (A7) are thus expressed by the coefficients as

$$\begin{cases} \lambda_0 \neq 0 \\ \lambda_1^2 - 4\lambda_2\lambda_0 \geq 0 \\ (\lambda_1 - \lambda_3\lambda_0)(\lambda_1\lambda_4 - \lambda_2\lambda_3) + (\lambda_4\lambda_0 - \lambda_2)^2 \geq 0 \\ \lambda_1(\lambda_1 - \lambda_3\lambda_0) + 2\lambda_0(\lambda_4\lambda_0 - \lambda_2) \leq 0 \end{cases} \cup \lambda_1^2 - 4\lambda_2\lambda_0 < 0 \tag{A8}$$

Finally, we can conclude that there is only one real solution to Eqs. (A1) if the coefficients satisfy the complementary condition of conditions (A6) and (A8).

Let

$$\lambda_0 = (1-e)[(2-e)k_1^2 + (1+e)(1-k_2)],$$
$$\lambda_1 = -2e(3-2e)k_1, \qquad \lambda_2 = 4e^2, \qquad \lambda_3 = -4k_1, \tag{A9}$$
$$\lambda_4 = -4$$

and substitute them into conditions (A6) and (A8). After combining the coefficients, we obtain the discriminants for the x–y plane:

$$\begin{cases} \Delta_0 = (2-e)k_1^2 - (1+e)(k_2-1) \neq 0 \\ \Delta_1 = k_1^2 - 4(1-e^2)(1-k_2) \\ \Delta_2 = (4-e^2)(1-e^2)k_1^4 - 2(2+e^2)(1-e^2)k_1^2k_2 + (4-7e^2)k_1^2 + (1-e^2)^2k_2^2 - 2(1-e^2)k_2 + 1 \\ \Delta_3 = -2(2-e^2)(1-e)(2-e)k_1^4 + 2(4-3e)(1-e^2)k_1^2k_2 - (8-6e-13e^2+12e^3-2e^4)k_1^2 - 2(1-e^2)^2k_2^2 + 2(1-e^2)(2-e^2)k_2 - 2(1-e^2) \end{cases} \tag{A10}$$

where Δ_0, Δ_1, Δ_2, and Δ_3 are equivalent to λ_0, Δ_a, $\Delta_+\Delta_-$, and $\Delta_+ + \Delta_-$, respectively. Similarly, let

$$\lambda_0 = (1-e)^2\{(1-k_1k_3)[(1+e) + (1-e)k_3^2] - [(1+e)k_2 + k_1k_3](1+k_3^2)\},$$
$$\lambda_1 = 2e(1-e)[(1+e)k_1 + (3-e)k_1k_3^2 + 2(1+e)k_2k_3], \tag{A11}$$
$$\lambda_2 = -4e^2[(1+e)k_2 + k_1k_3], \qquad \lambda_3 = 4k_3,$$
$$\lambda_4 = -4(1+e)/(1-e)$$

We can obtain the discriminants for the y–z plane

$$\Delta_0 = (2-e)k_1k_3^3 + (1+e)k_2k_3^2 + (2+e)k_1k_3 - (1-e)k_3^2 + (1+e)k_2 - 1 - e \tag{A12}$$

$$\Delta_1 = (1-e)^2k_1^2k_3^4 - 2(1+e^2)k_1^2k_3^2 + 4(1-e)k_1k_3^3 - 8(1+e)k_1k_2k_3 + 4(1-e^2)k_2k_3^2 + (1+e)^2k_1^2 - 4(1+e)^2k_2^2 + 4(1+e)k_1k_3 + 4(1+e)^2k_2 \tag{A13}$$

$$\begin{aligned}\Delta_2 = {} & (4-e^2)(1-e)^4k_1^2k_3^6 + 4(1+e)(1-e)^4k_1k_2k_3^5 \\ & + (1+e)(8-3e^2)(1-e)^3k_1^2k_3^4 - 4(1-e)^3k_1k_3^5 \\ & + (1+e)^2(1-e)^4k_2^2k_3^4 + 2(1+e)(1-e)^2(4-3e^2)k_1k_2k_3^3 \\ & - 2(1+e)(1-e)^3(1+e^2)k_2k_3^4 \\ & - 2(4-e^2)(1+e)(1-e)^2k_1k_3^3 + (4-11e^2+11e^4-3e^6)k_1^2k_3^2 \\ & + (1+e)^2(1-e)^4k_3^4 + 2(1-e^2)^2k_2^2k_3^2 \\ & + 2(1+e)(2-3e^2+2e^4)k_1k_2k_3 - 2(2+e^2)(1-e^2)^2k_2k_3^2 \\ & - e^2(1-e)(1+e)^3k_1^2 - 2(1-e)(1+e)^2(2-e^2)k_1k_3 \\ & + (1+e)^2k_2^2 + 2(1-e^2)^3k_3^2 - 2(1-e)(1+e)^3k_2 \\ & + (1+e)^4(1-e)^2\end{aligned} \tag{A14}$$

$$\begin{aligned}\Delta_3 = {} & -4(2-e)(1-e)^2k_1^2k_3^6 - 2(1+e)(4-e)(1-e)^2k_1k_2k_3^5 \\ & - (16-16e-13e^2+12e^3-e^4)k_1^2k_3^4 \\ & + 2(1-e)^2(4-e-e^2)k_1k_3^5 - 2(1-e^2)^2k_2^2k_3^4 \\ & - 2(1+e)(8-8e-5e^2+3e^3)k_1k_2k_3^3 \\ & + 4(1+e)(1-e)^2k_2k_3^4 + 2(1-e)(8+4e-5e^2-2e^3)k_1k_3^3 \\ & - (8+4e-10e^2-6e^3+2e^4)k_1^2k_3^2 \\ & - 2(1+e)^2(2-2e-e^2)k_2^2k_3^2 - 2(1+e)(1-e)^3k_3^4 \\ & - 2(1-e^2)(4+5e+2e^2)k_1k_2k_3 \\ & + 2(4+2e-e^2)(1-e^2)k_2k_3^2 + e^2(1+e)^2k_1^2 \\ & + 2(1+e)(4+e-3e^2-e^3)k_1k_3 - 2(1+e)^2k_2^2 \\ & - 4(1-e^2)^2k_3^2 + 2(2-e^2)(1+e)^2k_2 - 2(1+e)^3(1-e)\end{aligned} \tag{A15}$$

Acknowledgment

This work was supported by the National Natural Science Foundation of China (No. 10602027 and No. 10672084).

References

[1] Hill, G. W., "Researches in the Lunar Theory," *American Journal of Mathematics*, Vol. 1, No. 1, 1878, pp. 5–26. doi:10.2307/2369430

[2] Clohessy, W., and Wiltshire, R., "Terminal Guidance System for Satellite Rendezvous," *Journal of the Astronautical Sciences*, Vol. 27, No. 9, 1960, pp. 653–658, 674.

[3] London, H. S., "Second Approximation to the Solution of the Rendezvous Equations," *AIAA Journal*, Vol. 1, No. 7, 1963, pp. 1691–1693.

[4] Richardson, D. L., and Mitchell, J. W., "A Third-Order Analytical Solution for Relative Motion with a Circular Reference Orbit," *Journal of the Astronautical Sciences*, Vol. 51, No. 1, 2003, pp. 1–12.

[5] Gómez, G., and Marcote, M., "High-Order Analytical Solutions of Hill's Equations," *Celestial Mechanics and Dynamical Astronomy*, Vol. 94, No. 2, 2006, pp. 197–211. doi:10.1007/s10569-005-4821-2

[6] Lawden, D. F., *Optimal Trajectories for Space Navigation*, Butterworths, London, 1963, pp. 79–86.

[7] Tschauner, J., and Hempel, P., "Rendezvous zu ein min Elliptischer Bahn Umlaufenden Ziel," *Astronautica Acta*, Vol. 11, No. 2, 1965, pp. 104–109.

[8] Carter, T. E., "New Form for the Optimal Rendezvous Equations near a Keplerian Orbit," *Journal of Guidance, Control, and Dynamics*, Vol. 13, No. 1, 1990, pp. 183–186.

[9] Melton, R. G., "Time Explicit Representation of Relative Motion Between Elliptical Orbits," *Journal of Guidance, Control, and Dynamics*, Vol. 23, No. 4, 2000, pp. 604–610.

[10] Inalhan, G., Tillerson, M., and How, J. P., "Relative Dynamics and Control of Spacecraft Formations in Eccentric Orbits," *Journal of Guidance, Control, and Dynamics*, Vol. 25, No. 1, 2002, pp. 48–59.

[11] Schaub, H., and Alfriend, K. T., "J_2 Invariant Relative Orbits for Spacecraft Formations," *Celestial Mechanics and Dynamical Astronomy*, Vol. 79, No. 2, 2001, pp. 77–95. doi:10.1023/A:1011161811472

[12] Gim, D. W., and Alfriend, K. T., "State Transition Matrix of Relative Motion for the Perturbed Noncircular Reference Orbit," *Journal of Guidance, Control, and Dynamics*, Vol. 26, No. 6, 2003, pp. 956–971.

[13] Gim, D. W., and Alfriend, K. T., "Satellite Relative Motion Using Differential Equinoctial Elements," *Celestial Mechanics and Dynamical Astronomy*, Vol. 92, No. 4, 2005, pp. 295–336. doi:10.1007/s10569-004-1799-0

[14] Kasdin, N. J., Gurfil, P., and Kolemen, E., "Canonical Modelling of Relative Spacecraft Motion via Epicyclic Orbital Elements," *Celestial Mechanics and Dynamical Astronomy*, Vol. 92, No. 4, 2005, pp. 337–370. doi:10.1007/s10569-004-6441-7

[15] Karlgaard, C. D., and Lutze, F. H., "Second-Order Relative Motion Equations," *Journal of Guidance, Control, and Dynamics*, Vol. 26, No. 1, 2003, pp. 41–49.

[16] Baoyin, H., Li, J. F., and Gao, Y. F., "Dynamical Behaviors and Relative Trajectories of the Spacecraft Formation Flying," *Aerospace Science and Technology*, Vol. 6, No. 4, 2002, pp. 295–301. doi:10.1016/S1270-9638(02)01151-3

[17] Li, J. F., Meng, X., Gao, Y. F., and Li, X., "Study on Relative Orbital Configuration in Satellite Formation Flying," *Acta Mechanica Sinica*, Vol. 21, No. 1, 2005, pp. 87–94. doi:10.1007/s10409-004-0009-3

[18] Meng, X., Li, J. F., and Gao, Y. F., "Useful Relative Motion Description Method for Perturbations Analysis in Satellite Formation Flying," *Applied Mathematics and Mechanics*, Vol. 26, No. 11, 2005, pp. 1464–1474.

[19] Wang, H. M., Li, J. F., and Yang, W., "Solution Set on the Natural Satellite Formation Orbits Under First-Order Earth's Non-Spherical Perturbation," *Acta Mechanica Sinica*, Vol. 21, No. 5, 2005, pp. 503–510. doi:10.1007/s10409-005-0063-5

[20] Jiang, F. H., Li, J. F., and Baoyin, H., "Approximate Analysis for Relative Motion of Satellite Formation Flying in Elliptical Orbits," *Celestial Mechanics and Dynamical Astronomy*, Vol. 98, No. 1, 2007, pp. 31–66. doi:10.1007/s10569-007-9067-8

[21] Hughes, S. P., and Hall, C. D., "Optimal Configurations for Rotating Spacecraft Formations," *Journal of the Astronautical Sciences*, Vol. 48, Nos. 2–3, 2000, pp. 225–247.

[22] Schaub, H., "Relative Orbit Geometry Through Classical Orbit Element Differences," *Journal of Guidance, Control, and Dynamics*, Vol. 27, No. 5, 2004, pp. 839–848.

[23] Lane, C., and Axelrad, P., "Formation Design in Eccentric Orbits Using Linearized Equations of Relative Motion," *Journal of Guidance, Control, and Dynamics*, Vol. 29, No. 1, 2006, pp. 146–160.

[24] Kholshevnikov, K. V., and Vasiliev, N. N., "Natural Metrics in the Spaces of Elliptic Orbits," *Celestial Mechanics and Dynamical Astronomy*, Vol. 89, No. 2, 2004, pp. 119–125. doi:10.1023/B:CELE.0000034504.41897.ac

[25] Kholshevnikov, K. V., and Vasiliev, N. N., "On the Distance Function Between Two Keplerian Elliptic Orbits," *Celestial Mechanics and Dynamical Astronomy*, Vol. 75, No. 2, 1999, pp. 75–83. doi:10.1023/A:1008312521428

[26] Gurfil, P., and Kholshevnikov, K. V., "Manifolds and Metrics in the Relative Spacecraft Motion Problem," *Journal of Guidance, Control, and Dynamics*, Vol. 29, No. 4, 2006, pp. 1004–1010.

[27] Ilyin, V. A., and Poznyak, E. G., *Analytic Geometry*, translated from Russian, edited by Aleksanova, I., English Translation, Mir Publishers, Moscow, 1984, Chap. 7.